

Manuscript Number: ASR-D-14-00169R2

Title: The IONORT-ISP-WC system: inclusion of an electron collision frequency model for the D-layer

Article Type: SI: IRI and GNSS

Keywords: Ray-Tracing; Electron Density; IRI; Assimilative Modelling; Oblique Ionogram; Electron collision frequency model.

Corresponding Author: Dr. Alessandro Settimi, Ph.D

Corresponding Author's Institution: Istituto Nazionale di Geofisica e Vulcanologia (INGV)

First Author: Alessandro Settimi, Ph.D

Order of Authors: Alessandro Settimi, Ph.D; Marco Pietrella, Researcher; Michael Pezzopane, Researcher; Cesidio Bianchi, Technologist Supervisor

Abstract: The IONORT-ISP system (IONOspheric Ray-Tracing - IRI-SIRMUP-PROFILES) was recently developed and tested by comparing the measured oblique ionograms over the radio link between Rome (41.89°N, 12.48°E), Italy, and Chania (35.51°N, 24.02°E), Greece, with the IONORT-ISP simulated oblique ionograms (Settimi et al., 2013). The present paper describes an upgrade of the system to include: a) electron-neutral collision have been included by using a collision frequency model that consists of a double exponential profile; b) the ISP three dimensional (3-D) model of electron density profile grid has been extended down to the altitude of the D-layer; c) the resolution in latitude and longitude of the ISP 3-D model of electron density profile grid has been increased from 2°x2° to 1°x1°. Based on these updates, a new software tool called IONORT-ISP-WC (WC means with collisions) was developed, and a database of 33 IONORT-ISP-WC synthesized oblique ionograms calculated for single (1-hop paths) and multiple (3-hop paths) ionospheric reflections. The IONORT-ISP-WC simulated oblique ionograms were compared with the IONORT-IRI-WC synthesized oblique ionograms, generated by applying IONORT in conjunction with the International Reference Ionosphere (IRI) 3-D electron density grid, and the observed oblique ionograms over the aforementioned radio link. The results obtained show that (1) during daytime, for the lower ionospheric layers, the traces of the synthesized ionograms are cut away at low frequencies because of HF absorption; (2) during nighttime, for the higher ionospheric layers, the traces of the simulated ionograms at low frequencies are not cut off (very little HF absorption); (3) the IONORT-ISP-WC MUF values are more accurate than the IONORT-IRI-WC MUF values.

Dear Adv. Space Res. Past Editor in Chief, Dr. Peggy Ann Shea,  
this cover letter is for re-submitting our manuscript (ASR-D-14-00169), entitled as:

“The IONORT-ISP-WC system: inclusion of an electron collision frequency model for the D-layer”,

by the Authors,

Alessandro Settimi, Marco Pietrella, Michael Pezzopane, Cesidio Bianchi.

Please, let me know of your decision at your earliest convenience.

In attachments, You can find the word file of article, and the jpeg files of figures (dpi  $\geq$  600).

Moreover, we would like thanking the Reviewer 1 for his useful suggestions. We agree with him. We tried to change the paper in all the points that the Reviewer 1 has suggested. We have provided a detailed explanation in the attached reply letter.

Finally, in attachments, You can find a pdf file of the Reply to Reviewer 1.

With my best regards,  
Sincerely yours,  
Alessandro Settimi, PhD.

C:\Documents and Settings\Administrator\Desktop\[A-19]\Minor Revisions\Replies\Reply to Reviewer 1\Reply to Reviewer 1.doc

---

## **Second REVIEW OF:**

### **Testing the IONORT-ISP system, with the inclusion of an electron collision frequency model for the D-layer**

By

Alessandro Settimi, Marco Pietrella, Michael Pezzopane, Cesidio Bianchi

#### **1. Recommendations**

This paper has been re-worked enough that it can now be published, but with the indicated editorial changes.

I rewrote the abstract, on the grounds that this is the part of the paper that will be read by most readers.

#### **2. General Comments**

The convention is that the nose frequency on a real oblique ionogram is called the Maximum Observed Frequency (MOF). The term MUF could mean the instantaneous predicted value of the nose frequency (as in this paper) or the median nose frequency for a set of HF propagation predictions.

I still maintain that if you are going to compare calculated MUFs with MOFs from a physical system, you have to discuss SNR and antenna gains. But perhaps that would be the next step.

This paper deserves a mention: “McNamara, L. F., M. J. Angling, S. Elvidge, S. V. Fridman, M. A. Hausman, L. J. Nickisch, and L.-A. McKinnell (2013), *Assimilation procedures for updating ionospheric profiles below the F2 peak*, Radio Sci., 48, doi:10.1002/rds.20020.” The comparisons of the 1F MUFs and MOFs were based on Jones-type raytracing, but the authors considered this to be just another tool in their toolbox.

**Authors:** OK. We agree with the Reviewer 1. The revised manuscript was updated mentioning in the reference section the Mc Namara et al. (2013) article.

#### **3. Suggested Revised Abstract**

The IONORT-ISP system (IONOspheric Ray-Tracing – IRI-SIRMUP-PROFILES) that was recently developed and tested by comparing the measured oblique ionograms over the radio link between Rome (41.89°N, 12.48°E), Italy, and Chania (35.51°N, 24.02°E), Greece, with the IONORT-ISP simulated oblique ionograms [reference]. The present paper describes an upgrade of the system to include : a) electron -neutral collisions have been included by using a collision frequency model that consists of a double exponential profile; b) the ISP three dimensional (3-D) model of electron density profile grid has been extended down to the altitude of the D-layer; c) the resolution in latitude and longitude of the ISP 3-D model of electron density profile grid has been increased from 2°x2° to 1°x1°. Based on these updates, a new software tool called IONORT-ISP-WC (WC means with collisions) was developed, and a database of IONORT-ISP-WC synthesized oblique ionograms calculated for single (1-hop paths) and multiple (3-hop paths) ionospheric reflections was produced. The IONORT-ISP-WC simulated oblique ionograms were compared with the IONORT-IRI-WC synthesized oblique ionograms, generated by applying

IONORT in conjunction with the International Reference Ionosphere (IRI) 3-D electron density grid, and the observed oblique ionograms over the Rome to Chania path. The results obtained show that (1) during daytime, for the lower ionospheric layers, the traces of the synthesized ionograms are cut away at low frequencies **because of HF absorption**; (2) during night-time, for the higher ionospheric layers, the traces of the simulated ionograms at low frequencies are not cut off (**very little HF absorption**); (3) the IONORT-ISP-WC MUF values are more accurate than the IONORT-IRI-WC MUF values.

**Authors:** OK. We agree with the Reviewer 1. The revised manuscript was updated rewriting the abstract, and including the reference, as suggested.

#### 4. Small Revisions

Small font size indicates that this text is to be removed.

2/36 management of HF radio communications, and the predictions of **the** operating frequencies, are

2/56 of the wave along the **path, and** other optional quantities such as absorption, polarization, etc. The

2/61 Croft and Gregory, 1963; Jones, 1966) **ran** on old mainframes **that provided** only a numerical output. *They were not “old” – they were very modern.*

3/2 Cannon (1997) developed a two dimensional (2-D) analytic ray-tracing method called SMART **for**

3/10 ray-trace through complicated horizontal gradients along **and in** the direction of the ray path.

3/17 for **a** real-time use.

3/19 Recently an applicative software tool package named IONORT (IONOspheric Ray-Tracing), able to

3/20 work both with analytical and numerical electron density models, **was** developed at the Istituto

3/24,26 HF **waves propagating** in the

3/29 The **validity** of IONORT

4/0 the INGV, the IRI-SIRMUP-PROFILES (ISP) **model, capable** of providing a 3-D electron density

4/2 profile representation of the ionosphere in quasi real **time, was** developed.

4/17 Recently IONORT was used in conjunction with two kinds of 3-D electron density grids: **one**

4/39 **shown** that the ISP model can more accurately represent real conditions in the ionosphere than the

4/48 between electrons and neutral particles, consisting **of a** double exponential profile (Jones and

4/53 were made; the ISP electron density profile grid is also modified **starting now** **with** the D-layer

5/5 examples of the IONORT-ISP-WC synthesized oblique ionograms are shown and discussed in **terms**

5/12 the IONORT-ISP system. We describe our results in Section 3.

5/41 There is a large number of electron collision frequency models, for example constant collision

5/42 frequency, and exponential and tabular profiles (see references there in Jones and Stephenson,

6/2 electrons and neutrals for the D-layer that consists of a double exponential profile (Jones and

6/15 Would you care to explain the physics behind the two separate slopes?

6/47 COMPLEIK is just as reliable as ICEPAC, with the advantage of being implemented more GREEN highlighting?? YUK!

6/51 profiles corresponding to the COMPLEIK are just as reliable as the ICEPAC formula, for

7/0 In order to plot the ionogram with and without absorption, each Each synthesized ionogram was

7/22 by a typical absorption coefficient, i.e.  $L \leq 20$  dB, but does not show the trace of E-layer with a

7/32 This section discusses some examples of the ray path calculated by means of the proposed IONORTISP-WC system, and some results obtained by comparing the IONORT-ISP-WC synthesized oblique ionograms with the IONORT-IRI-WC synthesized oblique ionograms and the oblique ionograms measured along the Rome-Chania radio link are also discussed.

7/56 were either noisy or characterized by interference phenomena preventing users from accurately

8/24 ISP model ( $-10^\circ - 40^\circ$  in longitude,  $30^\circ - 50^\circ$  in latitude). The ray paths were calculated taking into

8/56 Fig. 3 shows an example of an oblique ionogram recorded over the Rome-Chania radio link on 07 July

9/5 The case of Fig. 3 shows clearly that the inclusion of the electron collision frequency model for the

9/10 low frequencies for the lower ionospheric layer (E region). As expected, both for 1-hop paths and 3-

9/36 MHz in case of WC; in this case a trace 6.8 MHz long is missing because of absorption suffered by

9/46 It must be noted that the MUF values calculated with or without the collisions model, in all the

9/48 cases analyzed show always the same value when a given electron density model is applied (IRI or

10/5-7 comprehensive comparison, no-collision (NC) cases are also included the cases obtained without applying the collisional model of Eq. 1 which are indicated with NC.

10/12 when the absorption of the propagating wave through the ionosphere can be considered negligible

10/29 practically occurs for the epoch 26 June 2011 at 01:00 UT where only very small differences are

10/56 and the measured MUF values. From the results shown in the columns D and E, it can be seen that

11/14 Fig. 5 the green squares marked with the symbol \*) is the performance of IONORT-IRI-WC is better

10/29 on the whole **database, it emerges** that the IONORT-ISP-WC MUF values are more accurate than the

10/51 **Gibilmanna, and** the only reference ionospheric station contributing to the ISP grids was Athens.

12/14 IONORT-ISP-WC system in providing **consistent** results.

**Authors:** OK. We agree with the Reviewer 1. The revised manuscript was updated including all these small revisions throughout the text body.

# The IONORT-ISP-WC system: inclusion of an electron collision frequency model for the D-layer

Alessandro Settimi<sup>a,\*</sup>, Marco Pietrella<sup>a</sup>, Michael Pezzopane<sup>a</sup>, Cesidio Bianchi<sup>a</sup>

<sup>a</sup>Istituto Nazionale di Geofisica e Vulcanologia, Via di Vigna Murata 605, 00143, Rome, Italy

\* Corresponding author: Alessandro Settimi; Tel: +39-06-51860719; Fax: +39-06-51860397; Email: [alessandro.settimi@ingv.it](mailto:alessandro.settimi@ingv.it);

Co-authors email addresses:

Marco Pietrella: [marco.pietrella@ingv.it](mailto:marco.pietrella@ingv.it);

Michael Pezzopane: [michael.pezzopane@ingv.it](mailto:michael.pezzopane@ingv.it);

Cesidio Bianchi: [cesidio.bianchi@ingv.it](mailto:cesidio.bianchi@ingv.it);

## Abstract

The IONORT-ISP system (IONOspheric Ray-Tracing – IRI-SIRMUP-PROFILES) was recently developed and tested by comparing the measured oblique ionograms over the radio link between Rome (41.89°N, 12.48°E), Italy, and Chania (35.51°N, 24.02°E), Greece, with the IONORT-ISP simulated oblique ionograms (Settimi et al., 2013). The present paper describes an upgrade of the system to include: a) electron-neutral collision have been included by using a collision frequency model that consists of a double exponential profile; b) the ISP three dimensional (3-D) model of electron density profile grid has been extended down to the altitude of the D-layer; c) the resolution in latitude and longitude of the ISP 3-D model of electron density profile grid has been increased from  $2^\circ \times 2^\circ$  to  $1^\circ \times 1^\circ$ . Based on these updates, a new software tool called IONORT-ISP-WC (WC means with collisions) was developed, and a database of 33 IONORT-ISP-WC synthesized oblique ionograms calculated for single (1-hop paths) and multiple (3-hop paths)

1 ionospheric reflections. The IONORT-ISP-WC simulated oblique ionograms were compared with  
2 the IONORT-IRI-WC synthesized oblique ionograms, generated by applying IONORT in  
3 conjunction with the International Reference Ionosphere (IRI) 3-D electron density grid, and the  
4 observed oblique ionograms over the aforementioned radio link. The results obtained show that (1)  
5 during daytime, for the lower ionospheric layers, the traces of the synthesized ionograms are cut  
6 away at low frequencies because of HF absorption; (2) during night-time, for the higher ionospheric  
7 layers, the traces of the simulated ionograms at low frequencies are not cut off (very little HF  
8 absorption); (3) the IONORT-ISP-WC MUF values are more accurate than the IONORT-IRI-WC  
9 MUF values.  
10  
11  
12  
13  
14  
15  
16  
17  
18  
19  
20  
21  
22  
23

24 **Keywords:** Ray-Tracing; Electron Density; IRI; Assimilative Modelling; Oblique Ionogram;  
25 Electron collision frequency model.  
26  
27  
28  
29  
30

## 31 1. Introduction

32 Ionospheric ray-tracing is a technique used to determine the path of a high frequency (HF)  
33 radio wave propagating in the ionosphere from a transmitting point to a receiving point.  
34  
35

36 Over the horizon radar systems, single station location, HF direction finding systems, the  
37 management of HF radio communications, and the predictions of operating frequencies, are  
38 examples of the main applications of ray-tracing, where a detailed knowledge of radio wave  
39 propagation through the ionosphere is needed.  
40  
41  
42  
43  
44  
45  
46  
47

48 Accurate ray-tracing is usually performed using numerical techniques requiring Haselgrove's  
49 equations (Haselgrove, 1955; Haselgrove and Haselgrove, 1960). The propagation of the wave, i.e.,  
50 the ray path, is described by six differential equations where the parameters of both the position and  
51 ray direction need to be integrated simultaneously at each point along the ray path. The integration  
52 provides the coordinates reached by the wave vector and its three components, the group time delay  
53 of the wave along the path, and other optional quantities such as absorption, polarization, etc. The  
54  
55  
56  
57  
58  
59  
60  
61  
62  
63  
64  
65



1 first ray-tracing algorithms developed in the 1960s (Dudziak, 1961; Lawrence and Posakony, 1961;  
2 Croft and Gregory, 1963; Jones, 1966) ran on old mainframes that provided only a numerical  
3  
4 output. Since then, many other ray-tracing programs have been developed. For example, Norman  
5  
6 and Cannon (1997) developed a two dimensional (2-D) analytic ray-tracing method called SMART  
7  
8 for which computer run times are about 10 times faster than those of numerical ray-tracing  
9  
10 packages. SMART automatically segments the ionosphere in terms of ground range and it is able to  
11  
12 accurately ray-trace through complicated horizontal gradients along the direction of the ray path.  
13  
14 Nowadays, the modern ray-tracing procedures (Coleman, 1998; Nickisch, 2008) have been  
15  
16 optimized and adapted to over the horizon radar applications using powerful computers and devices  
17  
18 for real-time use.  
19  
20  
21  
22

23  
24 Recently an applicative software tool package named IONORT (IONOspheric Ray-Tracing), able to  
25  
26 work both with analytical and numerical electron density models, was developed at the Istituto  
27  
28 Nazionale di Geofisica e Vulcanologia (INGV), for calculating a 3-D ray-trace for HF waves  
29  
30 propagating in the ionospheric medium (Azzarone et al., 2012).  
31  
32

33  
34 The validity of IONORT was checked by comparing at different frequencies the time delay of the  
35  
36 wave that results from the ray-tracing computation performed by IONORT ( $t_{\text{calc}}$ ), and the time delay  
37  
38 of the wave propagating along the oblique virtual path at the speed of light ( $t_{\text{virt}}$ ). It was found that  
39  
40 the IONORT ray-tracing algorithm fits nearly perfectly the theory so that the relative error  $\Delta t = t_{\text{calc}}$   
41  
42 -  $t_{\text{virt}}$  is only due to the discrete integration step (Bianchi et al., 2011).  
43  
44  
45

46 Ray-tracing can generally be performed accurately if the 3-D electron density distribution between  
47  
48 the transmitter and the receiver is known (Kashcheyev et al., 2012). A comprehensive specification  
49  
50 of the ionosphere in terms of electron density, neutral particles – electrons collision frequency, and  
51  
52 geomagnetic field is required in order to carry out an accurate ray-tracing. Therefore, when dealing  
53  
54 with near real-time applications of ray-tracing, it is of crucial importance to have a realistic  
55  
56 ionospheric modelling through 3-D models of ionospheric electron density, which after assimilating  
57  
58 measured data calculate an updated 3-D image of the ionosphere (Angling and Khattatov, 2006;  
59  
60  
61  
62  
63  
64  
65

1 Thompson et al., 2006; Fridman et al., 2006, 2009; Decker and McNamara, 2007; McNamara et al.,  
2 2007, 2008, 2010, 2011, 2013; Angling and Jackson-Booth, 2011; Shim et al., 2011). More  
3  
4 recently, at the INGV, the IRI-SIRMUP-PROFILES (ISP) model, capable of providing a 3-D  
5  
6 electron density profile representation of the ionosphere in quasi real time, was developed.  
7

8  
9 The ISP model has proven very effective in providing reliable electron density profiles under quiet  
10  
11 and disturbed geomagnetic conditions in several studies (Pezzopane et al., 2011, 2013). In particular  
12  
13 at the solar terminator, the electron densities calculated by the ISP model more accurately  
14  
15 represented the real conditions of the ionosphere than electron densities calculated using the  
16  
17 climatological IRI-URSI model alone.  
18

19  
20 Recently IONORT was used in conjunction with two kinds of 3-D electron density grids: one  
21  
22 generated by the International Reference Ionosphere (IRI) electron density model; and the other one  
23  
24 outputted by the ISP model (Pezzopane et al., 2011) after assimilating autoscaled foF2 and  
25  
26 M(3000)F2 data, and real-time vertical electron density profiles from the reference stations of Rome  
27  
28 (41.8°N, 12.5°E), Gibilmanna (37.9°N, 14.0°E) in Italy, and Athens (38.0°N, 23.5°E) in Greece.  
29  
30

31  
32 Synthesized oblique ionograms over the radio link between Rome and Chania (35.51°N, 24.02°E),  
33  
34 Greece, were produced by the IONORT-IRI and IONORT-ISP system and compared with the  
35  
36 measured oblique ionograms (Settimi et al., 2013). The comparisons carried out both in terms of the  
37  
38 ionogram shape and the maximum usable frequency (MUF) characterizing the radio path have  
39  
40 shown that the ISP model can more accurately represent real conditions in the ionosphere than the  
41  
42 IRI model, and that the ray-tracing results computed by IONORT are reasonably reliable.  
43  
44  
45

46  
47 The present paper is inspired by the abovementioned Settimi et al. (2013) study. With the aim of  
48  
49 extending this study, the IONORT-ISP system was upgraded including a collision frequency model  
50  
51 between electrons and neutral particles, consisting of a double exponential profile (Jones and  
52  
53 Stephenson, 1975). Moreover, some changes with respect to the previous version of the ISP model  
54  
55 were made; the ISP electron density profile grid is also modified starting now with the D-layer  
56  
57 (starting point at 65 km) and increasing the resolution in latitude and longitude from 2° x 2° to 1° x 1°.  
58  
59  
60  
61  
62

1 On the basis of these updates, a new software tool package, to which we refer hereafter as  
2 IONORT-ISP-WC (WC, means with collisions), was developed and a database of 33 IONORT-ISP-  
3 WC synthesized oblique ionograms completed with single (1-hop paths) and multiple (3-hop paths)  
4 ionospheric reflections was produced over the same radio link aforementioned. Some representative  
5 examples of the IONORT-ISP-WC synthesized oblique ionograms are shown and discussed in  
6 terms of comparison with the IONORT-IRI-WC synthesized oblique ionograms and the observed  
7 oblique ionograms. Section 2 describes the electron collision frequency model for the D-layer  
8 included in the IONORT-ISP system. We describe our results in Section 3. Concluding remarks and  
9 possible future developments are summarized in section 4.  
10  
11  
12  
13  
14  
15  
16  
17  
18  
19  
20  
21  
22  
23

## 24 **2. Description of the electron collision frequency model for the D-layer**

25 Collisions of free electrons with neutrals, heavy ions, or other electrons are important causes  
26 of various macroscopic phenomena. Electron collisions play an important role in the absorption of  
27 radio waves at lower altitudes (D-layer) (Settimi et al., 2014). Using an appropriate theory (Davies,  
28 1990) it is possible to deduce the electron collision frequency from radio wave propagation data.  
29 According to Budden (1965), for a detailed quantitative interpretation of some experiments it is  
30 necessary to apply the generalized theory (Sen and Wyller, 1960), while for most practical radio  
31 propagation problems, the classical theory (Appleton and Chapman, 1932) is adequate, especially  
32 when appropriate values are available for the effective electron collision frequency.  
33  
34  
35

36 There is a large number of electron collision frequency models, for example constant collision  
37 frequency, and exponential and tabular profiles (see references in Jones and Stephenson, 1975). It  
38 should be noted that if users want to implement other collision frequency models, they must write a  
39 subroutine to calculate the normalized frequency  $Z = \nu / 2\pi f$  (where  $\nu$  is the collision frequency  
40 between electrons and neutral air molecules, and  $f$  is the transmitted wave frequency) and its  
41 gradients ( $\partial Z / \partial r$ ,  $\partial Z / \partial \theta$ ,  $\partial Z / \partial \varphi$ ) as a function of position within spherical polar coordinates ( $r$ ,  $\theta$ ,  $\varphi$ )  
42  
43  
44  
45  
46  
47  
48  
49  
50  
51  
52  
53  
54  
55  
56  
57  
58  
59  
60  
61  
62  
63  
64  
65

1 referring to a system of computational coordinates (which is not necessarily the same as geographic  
2 coordinates).

3  
4 The current version of the IONORT-ISP-WC system includes a collision frequency model between  
5 electrons and neutrals for the D-layer that consists of a double exponential profile (Jones and  
6  
7 Stephenson, 1975)  
8  
9

$$10 \quad \nu(h) = \nu_1 e^{-a_1(h-h_1)} + \nu_2 e^{-a_2(h-h_2)}, \quad (1)$$

11  
12  
13  
14  
15  
16  
17  
18  
19 where  $\nu$  is the collision frequency at the height above ground  $h$ . The first exponential has the  
20 following specifications: collision frequency at height  $h_1$ ,  $\nu_1=3.65 \cdot 10^4$  collisions per second;  
21  
22 reference height,  $h_1=100$  km; exponential decrease of  $\nu$  with height,  $a_1=0.148$  km<sup>-1</sup>. The second  
23  
24 exponential has the following specifications: collision frequency at height  $h_2$ ,  $\nu_2=30$  collisions per  
25  
26 second; reference height,  $h_2=140$  km; exponential decrease of  $\nu$  with height,  $a_2=0.0183$  km<sup>-1</sup>. Fig. 1  
27  
28 shows the trend of the electron collision frequency implemented in the IONORT-ISP-WC system.  
29  
30  
31

32  
33  
34 It should be noted that, in Settini et al. (2014) paper, simple complex eikonal equations, in quasi-  
35  
36 longitudinal (QL) approximation (Rawer, 1976), for calculating the non-deviative absorption  
37  
38 coefficient due to the propagation across the D-layer were encoded into a so called COMPLEIK  
39  
40 (COMPLEx EIKonal) subroutine of the IONORT program. The IONORT program already included  
41  
42 the same electron collision frequency model for the D-layer, consisting of the double exponential  
43  
44 profile (Jones and Stephenson, 1975). As main outcome of that paper, the simple COMPLEIK  
45  
46 algorithm was compared to the more elaborate semi-empirical ICEPAC formula (Stewart, undated).  
47  
48  
49 COMPLEIK is just as reliable as ICEPAC, with the advantage of being implemented more directly.  
50  
51  
52 Settini et al. (2014), applying just Eq. 1 (Fig. 1), proved that, the non-deviative absorption profiles  
53  
54 corresponding to COMPLEIK are just as reliable as the ICEPAC formula, for all the ordinary and  
55  
56 extraordinary rays effectively radio linking Rome and Chania. Instead, the absorption profiles  
57  
58  
59  
60  
61  
62  
63  
64  
65

1  
2  
3  
4  
5  
6  
7  
8  
9  
10  
11  
12  
13  
14  
15  
16  
17  
18  
19  
20  
21  
22  
23  
24  
25  
26  
27  
28  
29  
30  
31  
32  
33  
34  
35  
36  
37  
38  
39  
40  
41  
42  
43  
44  
45  
46  
47  
48  
49  
50  
51  
52  
53  
54  
55  
56  
57  
58  
59  
60  
61  
62  
63  
64  
65

corresponding to the COMPLEIK subroutine lose their reliability just for all the rays that cannot establish the radio link Rome-Chania.

Each synthesized ionogram was computed with or without applying the electron collision frequency model. For the sake of clarity, the synthesized ionograms are generated considering only the ordinary trace and taking into account the geomagnetic field.

For all cases, with the exclusion of those at the solar terminator and during the night, an oblique ionogram computed without applying the electron collision frequency model (1) consists of (e.g., Settimi et al., 2014): 1) a trace for the ionospheric F1-F2 layers at high altitudes ( $h > 150$  km); 2) a trace for the E-layer at lower altitude ( $90 \text{ km} < h \leq 150 \text{ km}$ ). Generally, an ionogram computed applying the electron collision frequency model (1) shows the trace of F1-F2 layers, characterized by a typical absorption coefficient, i.e.  $L \leq 20$  dB, but does not show the trace of E-layer with a higher absorption coefficient, i.e.  $L \gg 20$  dB (e.g., McNamara, 1991).

### 3. Results and Discussion

This section discusses some examples of the ray path calculated by means of the proposed IONORT-ISP-WC system and some results obtained by comparing the IONORT-ISP-WC synthesized oblique ionograms with the IONORT-IRI-WC synthesized oblique ionograms and the oblique ionograms measured along the Rome-Chania radio link. The database of the observed oblique ionograms used in this study, is constituted by 33 oblique ionograms recorded over the Rome-Chania radio link in June, July, and October 2011 in the daytime, night-time, at sunrise, and at sunset during quiet and moderate geomagnetic activity.

The ionograms comprising this database were selected on the criteria of: a) clarity of trace, which is essential in order to perform a trace shape comparison between measured and synthesized ionograms. In this respect it is worth noting that often the recorded Rome-Chania radio link traces were either noisy or characterized by interference phenomena preventing users from accurately validating the MUF, in addition to not being tagged for polarization; b) most of the ionograms had

1 to be recorded at specific times for which both the Athens autoscaling, and at least one between the  
2 Rome and Gibilmanna autoscalings were available and essentially correct. These “boundary  
3 conditions” greatly limited the number of measured oblique ionograms in the test database. The b)  
4 requirement is necessary to guarantee that the assimilation process was properly performed with  
5 data from at least two ionospheric stations located close to the two extremities of the radio path. It  
6 will be seen in Section 4 that the assimilation of data from only one station at only one extremity of  
7 the radio path can cause significant underestimation/overestimation of the real MUF.  
8

9 Fig. 2 shows four examples of the IONORT’s graphical user interface (for a more detailed  
10 description of this interface, see Azzarone et al., 2012).  
11

12 Each example shows the 2-D (at the bottom) and 3-D (on the right side) ray paths along the Rome-  
13 Chania radio link (azimuth angle equal to  $121.6^\circ$ ), which falls beyond the validity area of regional  
14 ISP model ( $-10^\circ - 40^\circ$  in longitude,  $30^\circ - 50^\circ$  in latitude). The ray paths were calculated taking into  
15 account the geomagnetic field, the electron collision frequency model for the D-layer (Eq. 1), and  
16 the electron density profile grid calculated at the epoch 26 June 2011 at 01:00 UT by the global IRI  
17 model.  
18

19 It must be noted that the IONORT-IRI-WC system, with respect to the previous version IONORT-  
20 IRI, is now able to provide ray paths also with multiple (3-hop paths) ionospheric reflections, as  
21 shown for the two cases depicted at the bottom of Fig. 2.  
22

23 In all the synthesized ionograms with single or multiple ionospheric reflections (1 – 3 hop paths),  
24 even though the ionosphere is not characterized by large horizontal gradients, a nested loop cycle  
25 was iterated with azimuth angles from  $121^\circ$  to  $122^\circ$  of step  $0.2^\circ$ . The elevation angle step was set to  
26  $0.2^\circ$  and the receiver (RX) range accuracy to 0.1 % (for a more detailed description of how the  
27 parameters, i.e. azimuth, elevation steps and RX range accuracy, are used in the ray-tracing  
28 program, we refer the reader to Appendix A of Settimi et al., 2013).  
29

30 Fig. 3 shows an example of an oblique ionogram recorded over the Rome-Chania radio link on 07  
31 July 2011 at 15:00 UT (top panel), and its corresponding synthesized ionograms generated by the  
32  
33  
34  
35  
36  
37  
38  
39  
40  
41  
42  
43  
44  
45  
46  
47  
48  
49  
50  
51  
52  
53  
54  
55  
56  
57  
58  
59  
60  
61  
62  
63  
64  
65

1 IONORT-IRI-WC (middle panel) and IONORT-ISP-WC (bottom panel) system. The cases labelled  
2 with NC (NC means No Collisions) obtained without including the electron collision frequency  
3 model for the D-layer (Eq. 1) are also shown for a further and more comprehensive comparison.  
4

5  
6  
7 The case of Fig. 3 shows clearly that the inclusion of the electron collision frequency for the D-  
8 layer during daytime has the effect of cutting away the trace of the synthesized ionogram at the low  
9 frequencies for the lower ionospheric layer (E region). As expected, both for 1-hop paths and 3-hop  
10 paths, the Lowest Observed Frequencies (LOF) calculated not taking into account the collisional  
11 model, both in case of IRI and ISP electron density profile grids, are systematically much smaller  
12 than those calculated when the collisional model provided by the Eq. 1 is applied. More precisely  
13 looking at 1-hop paths, for IRI electron density profile grids (see second panel of Fig. 3),  $LOF_E =$   
14 4.2 MHz with NC and  $LOF_E = 10.0$  MHz in case of WC, so that a trace long 5.8 MHz is cut off  
15 because of absorption; for the higher ionospheric layer (F region)  $LOF_F = 5.6$  MHz with NC and  
16  $LOF_F = 5.5$  MHz in case of WC, which means that the trace is not cut off. This is also an expected  
17 result because at the height of F region the effect of the collisions is less important and therefore the  
18 waves propagating at a given frequency do not suffer an important absorption. For ISP electron  
19 density profile grids (see third panel of Fig. 3),  $LOF_E = 3.1$  MHz with NC and  $LOF_E = 9.9$  MHz in  
20 case of WC; in this case a trace 6.8 MHz long is missing because of absorption suffered by the  
21 wave propagating at the height of E region. Again, at higher heights the effect of the collisions on  
22 the propagating waves can be considered negligible because the calculated LOF values are similar  
23 being  $LOF_F = 9.0$  MHz with NC and  $LOF_F = 8.8$  MHz in case of WC.  
24  
25  
26  
27  
28  
29  
30  
31  
32  
33  
34  
35  
36  
37  
38  
39  
40  
41  
42  
43  
44  
45  
46  
47

48 It must be noted that the MUF values calculated with or without the collisions, in all the cases  
49 analyzed show the same value when a given electron density model is applied (IRI or ISP); this is a  
50 reasonable result because MUF depends only on the highest frequency reflected by the F2-layer,  
51 (foF2), and the secant of the optimum angle at which to broadcast a signal that is to be received at a  
52 given distance  $D$ , (M(D)F2).  
53  
54  
55  
56  
57  
58  
59  
60  
61  
62  
63  
64  
65

1 The two cases in Fig. 4 show an example of oblique ionograms recorded over the Rome-Chania  
2 radio link on 9 October 2011 at 03:00 UT (at the top, on the left), and 26 June 2011 at 01:00 UT (at  
3 the top, on the right) with their corresponding synthesized ionograms generated by the IONORT-  
4 IRI-WC (middle panels) and IONORT-ISP-WC (bottom panels). For a further and more  
5 comprehensive comparison, no-collision (NC) cases are also included.  
6  
7

8 It should be noted that these two examples are relative to ionograms observed during night-time  
9 when the absorption of the propagating wave through the ionosphere can be considered negligible  
10 because of the lack of the lower absorbing layers (D and E regions). For this reason, the  $LOF_F$   
11 calculated with or without the electron collision frequency model for the D-layer show practically  
12 the same values. To better clarify this feature, we can refer to the legends of Fig. 4 where the  $LOF_F$   
13 values are reported. For the epoch 9 October 2011 at 03:00 UT, both for IRI and ISP electron  
14 density profile grids (see second and third panel of Fig. 4 respectively), the  $LOF_F$  values calculated  
15 with or without the collisional model are equal to 3.0 MHz for 1-hop and 3-hop paths. The same  
16 occurs for the epoch 26 June 2011 at 01:00 UT where only very small differences are observed  
17 between the  $LOF_F$  calculated with NC and the  $LOF_F$  obtained in the case WC: discrepancies of 0.1  
18 MHz (for 3-hop paths) and 0.4 MHz (for 1-hop paths) are observed when the IRI and ISP electron  
19 density profile grids are considered respectively, which means that during night-time the simulated  
20 ionograms do not show traces cut away at lower frequencies.  
21  
22

23 The results of this study are summarized in Tab. 1 where is shown the full database concerning the  
24 epochs for which the observed ionograms over the radio link Rome-Chania were selected according  
25 to the criteria a) and b) above mentioned.  
26  
27

28 The MUF calculated by both the IONORT-IRI-WC and the IONORT-ISP-WC system, and the  
29 measured MUF for all the ionograms of the test database, are shown together with the  
30 corresponding differences between the modelled (IONORT-IRI-WC or IONORT-ISP-WC system)  
31 and the measured MUF values. From the results shown in the columns D and E, it can be seen that  
32 IONORT-ISP-WC MUF values are close to the measured values in most of the cases considered.  
33  
34  
35  
36  
37  
38  
39  
40  
41  
42  
43  
44  
45  
46  
47  
48  
49  
50  
51  
52  
53  
54  
55  
56  
57  
58  
59  
60  
61  
62  
63  
64  
65



1 To better highlight the results of Tab. 1, the results of the comparison between the differences  
2 (IONORT-IRI-WC MUF – measured MUF), and (IONORT-ISP-WC MUF – measured MUF), are  
3  
4 also presented in Fig. 5 for the whole test database. It is clearly evident that IONORT-ISP-WC  
5  
6 system performs better than IONORT-IRI-WC system because in most of cases considered, the  
7  
8 differences (IONORT-ISP-WC MUF – measured MUF) are very small (in particular, see in Fig. 5  
9  
10 the red squares ranged between the horizontal lines -0.5 – 0.5 MHz), and only in six cases (see in  
11  
12 Fig. 5 the green squares marked with the symbol \*) is the performance of IONORT-IRI-WC better  
13  
14 than that of IONORT-ISP-WC.  
15  
16  
17  
18  
19  
20  
21

#### 22 **4. Conclusions and future developments**

23  
24 The oblique ionograms synthesized by the IONORT-ISP-WC system are generally better than  
25  
26 the oblique ionograms synthesized by the IONORT-IRI-WC system. From the analysis conducted  
27  
28 on the whole database, it emerges that the IONORT-ISP-WC MUF values are more accurate than  
29  
30 the IONORT-IRI-WC MUF values (see Tab. 1 and Fig. 5). As expected, this means that the  
31  
32 representation of the ionosphere produced by the ISP model is more realistic than the climatological  
33  
34 representation produced by the IRI model, and also that the ray-tracing results performed by the  
35  
36 IONORT algorithm are reasonably reliable.  
37  
38  
39  
40

41 Nevertheless, Tab. 1 and Fig. 5 show also some cases for which the MUF values provided by the  
42  
43 IONORT-ISP-WC system are greatly underestimated, on 8 October 2011 at 19: 00 UT and, most  
44  
45 noticeably, on 8 October 2011 at 10.30 UT, or overestimated, on 6 July 2011 at 12:00 UT, and 9  
46  
47 October 2011 at 05:00 and 06:30 UT. In these cases no data was available from Rome and  
48  
49 Gibilmanna, and the only reference ionospheric station contributing to the ISP grids was Athens.  
50  
51 This estimate of MUF values provided by the IONORT-ISP-WC system could probably be  
52  
53 smoothed out by including additional ionospheric reference stations in the region of interest, and  
54  
55 especially located around the midpoint of the path considered.  
56  
57  
58  
59  
60  
61  
62  
63  
64  
65

1  
2  
3  
4  
5  
6  
7  
8  
9  
10  
11  
12  
13  
14  
15  
16  
17  
18  
19  
20  
21  
22  
23  
24  
25  
26  
27  
28  
29  
30  
31  
32  
33  
34  
35  
36  
37  
38  
39  
40  
41  
42  
43  
44  
45  
46  
47  
48  
49  
50  
51  
52  
53  
54  
55  
56  
57  
58  
59  
60  
61  
62  
63  
64  
65

It is also worth noting that the comparison of the synthesized ionograms with or without the collisional model used in this study (see for example Figs. 3 and 4), shows that during daytime, for the lower ionospheric layers, the traces of the synthesized ionograms are cut away at low frequencies; during night-time, when the lower ionospheric layer are missing and the absorption is not important, the traces of the simulated ionograms for the higher ionospheric layers are not cut off at low frequencies. These results provide a further confirmation about the goodness of the IONORT-ISP-WC system in providing consistent results.

In summary, the results presented in this paper suggest that: a) the assimilation of data measured at multiple ionospheric reference stations by ISP is very important to obtain as reliable an image of the ionosphere as possible; b) the IONORT-ISP-WC system can be proposed as a valid tool for operational use.

With regard to future developments, the IONORT-ISP-WC system does not provide a procedure to compute the horizontal gradients of the ionosphere, although the electron density profile grids are now characterized by a denser resolution in the latitude and longitude coordinates, i.e. from  $2^\circ \times 2^\circ$  to  $1^\circ \times 1^\circ$ . This issue will be addressed in the future by developing a procedure capable of taking the presence of horizontal gradients into account, in order to improve the IONORT-ISP-WC system.

Moreover, more oblique sounding measurements will need to be conducted in order to investigate the issue of the underestimates/overestimates of MUF values and further test the behaviour of the IONORT-ISP-WC system.

## Acknowledgments

The authors are extremely grateful to Dr. Bruno Zolesi and Dr. Ljiljana Cander for the useful simulations generated by the SIRMUP model; Dr. Carlo Scotto for interesting pointers to literature regarding ionospheric models and ray-tracing; Dr. Enrico Zuccheretti, and Prof. J. Makris for their helpful discussions regarding oblique ionograms; and Dr. Alessandro Pignatelli for his valuable computer support.

## References

1  
2 Angling, M. J., and Jackson-Booth, N. K., A short note on the assimilation of collocated and  
3  
4 concurrent GPS and ionosonde data into the Electron Density Assimilative Model, *Radio Sci.*, 46  
5  
6 (6), RS0D13, doi:10.1029/2010RS004566, 2011.  
7  
8

9  
10  
11 Angling, M. J., and Khattatov., B., Comparative study of two assimilative models of the ionosphere,  
12  
13 *Radio Sci.*, 41 (5), RS5S20, doi:10.1029/2005RS003372, 2006.  
14  
15

16  
17  
18  
19 Appleton, E. V., and Chapman, F. W., The collisional friction experienced by vibrating electrons in  
20  
21 ionized air, *Proc. Phys. Soc., London*, 44 (3), 246–254, doi:10.1088/0959-5309/44/3/302, 1932.  
22  
23

24  
25  
26 Azzarone, A., Bianchi, C., Pezzopane, M., Pietrella, M., Scotto, C., and Settimi, A., IONORT: A  
27  
28 Windows software tool to calculate the HF ray tracing in the ionosphere, *Comp. Geosc.*, 42, 57-63,  
29  
30 doi:10.1016/j.cageo.2012.02.008, 2012.  
31  
32

33  
34  
35  
36 Bianchi, C., Settimi, A., Scotto, C., Azzarone, A., and Lozito, A., A method to test HF ray tracing  
37  
38 algorithm in the ionosphere by means of the virtual time delay, *Adv. Space Res.*, 48 (10), 1600–  
39  
40 1605, doi:10.1016/j.asr.2011.07.020, 2011.  
41  
42

43  
44  
45 Budden, K. G., Effect of electron collisions on the formulas of magnetoionic theory, *Radio Sci.*,  
46  
47 69D (2), 191-211, 1965.  
48  
49

50  
51  
52  
53 Coleman, C. J., A ray-tracing formulation and its application to some problems in over-the-horizon  
54  
55 radar, *Radio Sci.* 33 (4), 1187-1197, doi: 10.1029/98RS01523, 1998.  
56  
57

1 Croft, T. A., and Gregory, L., Stanford University, Stanford Electronics Laboratories, Fast, versatile  
2 ray-tracing program for IBM 7090 digital computers, Defense Technical Information Center (ed.),  
3  
4 Rept. SEL-63-107, TR 82, Contract no. 225 (64), Office of Naval Research, Advanced Research  
5  
6 Projects Agency, Stanford, California, USA, 28 pp., 1963.  
7  
8  
9

10  
11 Davies, K., Ionospheric Radio, Peter Peregrinus Ltd. (ed.) on behalf of the Institution of Electrical  
12  
13 Engineers (IET), London, UK, 508 pp., 1990.  
14  
15  
16

17  
18  
19 Decker, D. T., and McNamara, L. F., Validation of ionospheric weather predicted by Global  
20  
21 Assimilation of Ionospheric measurements (GAIM) models, Radio Sci., 42 (4), RS4017,  
22  
23 doi:10.1029/2007RS003632, 2007.  
24  
25  
26

27  
28  
29 Dudziak, W. F., Three-dimensional ray trace computer program for electromagnetic wave  
30  
31 propagation studies, Technical Military Planning Operation RM 61TMP-32, Defense Atomic  
32  
33 Support Agency DASA 1232 , General Electrical Company, Santa Barbara, California, USA, 170  
34  
35 pp., 1961.  
36  
37  
38

39  
40  
41 Fridman, S. V., Nickisch, L. J., Aiello, M., and Hausman, M., Real-time reconstruction of the three-  
42  
43 dimensional ionosphere using data from a network of GPS receivers, Radio Sci., 41 (5), RS5S12,  
44  
45 doi:10.1029/2005RS003341, 2006.  
46  
47  
48

49  
50  
51 Fridman, S. V., Nickisch, L. J., and Hausman, M., Personal-computer-based system for real-time  
52  
53 reconstruction of the three-dimensional ionosphere using data from diverse sources, Radio Sci., 44  
54  
55 (3), RS3008, doi:10.1029/2008RS004040, 2009.  
56  
57  
58

1 Haselgrove, J., Ray theory and a new method of ray tracing, Conference on the Physics of the  
2 Ionosphere, Proc. Phys. Soc. London, 23, 355-364, 1955.  
3  
4

5  
6  
7 Haselgrove, C. B., and Haselgrove, J., Twisted ray paths in the ionosphere, Proc. Phys. Soc.  
8  
9 London, 75 (3), 357-363, doi:10.1088/0370-1328/75/3/304, 1960.  
10

11  
12  
13  
14 Jones, R. M., A three dimensional ray tracing computer program, ESSA Tech. Rep., IER 17 - ITSA  
15  
16  
17 17, Government Printing Office, Washington, USA, 1966.  
18  
19

20  
21  
22 Jones, R. M., and Stephenson, J. J., A versatile three-dimensional ray tracing computer program for  
23  
24 radio waves in the ionosphere, OT Report, 75-76, U.S. Department of Commerce, Office of  
25  
26 Telecommunication, U.S. Government Printing Office, Washington, USA, 185 pp., 1975.  
27  
28

29  
30  
31 Kashcheyev, A., Nava, B., and Radicella, S. M., Estimation of higher-order ionospheric errors in  
32  
33 GNSS positioning using a realistic 3-D electron density model, Radio Sci., 47 (4), RS4008,  
34  
35  
36 doi:10.1029/2011RS004976, 2012.  
37  
38

39  
40  
41 Lawrence, R. S., and Posakony, D. J., A digital ray tracing program for ionospheric research, in  
42  
43 Proc. Intern. Space Sci. Symp., vol. 2, edited by H. C. van de Hulst, C. de Jager, and A. F. Moore,  
44  
45  
46 pp. 258-276, North Holland, Amsterdam, 1961.  
47  
48

49  
50  
51 McNamara, L. F. The Ionosphere: Communications, Surveillance, and Direction Finding (Orbit: A  
52  
53  
54 Foundation Series). Published by Krieger Pub Co, Hardcover, 248 pp., 1991.  
55  
56  
57  
58  
59  
60  
61  
62  
63  
64  
65

1 McNamara, L. F., Decker, D. T., Welsh, J. A., and Cole, D. G., Validation of the Utah State  
2 University Global Assimilation of Ionospheric Measurements (GAIM) model predictions of the  
3  
4 maximum usable frequency for a 3000 km circuit, *Radio Sci.*, 42 (3), RS3015,  
5  
6 doi:10.1029/2006RS003589, 2007.  
7  
8  
9

10  
11 McNamara, L. F., Baker, C. R., and Decker, D. T., Accuracy of USU-GAIM specifications of foF2  
12  
13 and M(3000)F2 for a worldwide distribution of ionosonde locations, *Radio Sci.*, 43 (1), RS1011,  
14  
15 doi:10.1029/2007RS003754, 2008.  
16  
17  
18

19  
20  
21 McNamara, L. F., Retterer, J. M., Baker, C. R., Bishop, G. J., Cooke, D. L., Roth, C. J., and Welsh,  
22  
23 J. A., Longitudinal structure in the CHAMP electron densities and their implications for global  
24  
25 ionospheric modelling, *Radio Sci.*, 45 (2), RS2001, doi:10.1029/2009RS004251, 2010.  
26  
27  
28

29  
30  
31 McNamara, L. F., Bishop, G. J., and Welsh, J. A., Assimilation of ionosonde profiles into a global  
32  
33 ionospheric model, *Radio Sci.*, 46 (2), RS2006, doi:10.1029/2010RS004457, 2011.  
34  
35  
36

37  
38  
39 McNamara, L. F., Angling, M. J., Elvidge, S., Fridman, S. V., Hausman, M. A., Nickisch, L. J., and  
40  
41 McKinnell, L.-A., Assimilation procedures for updating ionospheric profiles below the F2 peak,  
42  
43 *Radio Sci.*, 48 (2), 143-157, doi:10.1002/rds.20020, 2013.  
44  
45  
46

47  
48  
49 Nickisch, L. J., Practical Applications of Haselgrove's Equations for HF systems, *Radio Sci.*  
50  
51 *Bulletin*, 325, 36-48, 2008 ([http://www.ursi.org/files/RSBissues/RSB\\_325\\_2008\\_06.pdf](http://www.ursi.org/files/RSBissues/RSB_325_2008_06.pdf)).  
52  
53  
54

55  
56 Norman, R. J., and Cannon, P. S., A two-dimensional analytic ray tracing technique  
57  
58 accommodating horizontal gradients, *Radio Sci.*, 32 (2), 387-396, doi: 10.1029/96RS03200, 1997.  
59  
60  
61

1 Pezzopane, M., Pietrella, M., Pignatelli, A., Zolesi, B., and Cander, L. R., Assimilation of  
2 autoscaled data and regional and local ionospheric models as input sources for real-time 3-D  
3  
4 International Reference Ionosphere modelling, Radio Sci., 46 (5), RS5009,  
5  
6 doi:10.1029/2011RS004697, 2011.  
7  
8  
9

10  
11 Pezzopane, M., Pietrella, M., Pignatelli, A., Zolesi, B., and Cander, L. R., Testing the three-  
12  
13 dimensional IRI-SIRMUP-P mapping of the ionosphere for disturbed periods, Adv. Space Res., 52  
14  
15 (10), 1726-1736, doi: 10.1016/j.asr.2012.11.028, 2013.  
16  
17  
18  
19  
20

21 Rawer, K., Manual on ionospheric absorption measurements, Report UAG – 57, edited by K.  
22  
23 Raver, published by World Data Center A for Solar-Terrestrial Physics, NOAA, Boulder, Colorado,  
24  
25 USA, and printed by U.S. Department of Commerce National Oceanic and Atmospheric  
26  
27 Administration Environmental Data Service, Asheville, North Carolina, USA, 202 pp., 1976.  
28  
29  
30  
31  
32

33  
34 Sen, H. K., and Wyller, A. A., On the Generalization of the Appleton-Hartree Magnetoionic  
35  
36 Formulas, J. Geophys. Res., 65 (12), 3931-3950, doi:10.1029/JZ065i012p03931, 1960.  
37  
38  
39  
40

41 Settimi, A., Pezzopane, M., Pietrella, M., Bianchi, C., Scotto, C., Zuccheretti, E., Makris, J., Testing  
42  
43 the IONORT-ISP system: a comparison between synthesized and measured oblique ionograms,  
44  
45 Radio Science, 48 (2), 167-179, doi:10.1002/rds.20018, 2013.  
46  
47  
48  
49  
50

51 Settimi, A., Pietrella, M., Pezzopane, M., Zolesi, B., Bianchi, C., Scotto, C., The COMPLEIK  
52  
53 subroutine of the IONORT-ISP system for calculating the non-deviative absorption: A comparison  
54  
55 with the ICEPAC formula, Adv. Space. Res., 53 (2), 201-218, doi:10.1016/j.asr.2013.10.035, 2014.  
56  
57  
58  
59  
60  
61  
62  
63  
64  
65



1 Shim, J. S., Kuznetsova, M., Rastätter, L., et al.. CEDAR Electrodynamics Thermosphere  
2 Ionosphere (ETI) Challenge for systematic assessment of ionosphere/thermosphere models: NmF2,  
3 hmF2, and vertical drift using ground-based observations. Space Weather, 9 (12), S12003,  
4  
5 doi:10.1029/2011SW000727, 2011.  
6  
7  
8  
9

10  
11 Stewart, F. G., Ionospheric Communications Enhanced Profile Analysis & Circuit (ICEPAC)  
12 Prediction Program, Technical Manual, 91 pp., undated.  
13  
14  
15  
16  
17 ([http://elbert.its.blrdoc.gov/hf\\_prop/manuals/icepac\\_tech\\_manual.pdf](http://elbert.its.blrdoc.gov/hf_prop/manuals/icepac_tech_manual.pdf)).  
18  
19  
20

21 Thompson, D. C., Scherliess, L., Sojka, J. J., and Schunk, R. W., The Utah State University Gauss-  
22 Markov Kalman filter of the ionosphere: The effect of slant TEC and electron density profile data  
23 on model fidelity, J. Atmos. Solar-Terr. Phys., 68 (9), 947–958, doi:10.1016/j.jastp.2005.10.011,  
24  
25  
26  
27  
28  
29 2006.  
30  
31  
32  
33  
34  
35  
36  
37  
38  
39  
40  
41  
42  
43  
44  
45  
46  
47  
48  
49  
50  
51  
52  
53  
54  
55  
56  
57  
58  
59  
60  
61  
62  
63  
64  
65

1 **Figure 1.** Semi-logarithmic plot of the electron collision frequency  $\nu$ , in units of  $s^{-1}$ , as a function of  
2 height above ground  $h$ , in the range 50 – 250 km obtained from Eq. 1.  
3  
4  
5  
6

7 **Figure 2.** Graphical user interface of IONORT program. The 2-D and 3-D visualizations of the ray  
8 paths are shown at the bottom and right respectively, considering a transmitter point at Rome and an  
9 azimuth angle of transmission equal to  $121.6^\circ$  (direction of Chania), on 26 June 2011 at 01:00 UT.  
10  
11 To realize the full potential of IONORT, composite simulations, based on the global IRI model, are  
12 performed not only inside but also outside the central Mediterranean region, by taking the  
13 geomagnetic field and the electron collisions into account, with single or multiple ionospheric  
14 reflections (1 – 3 hop paths): for a fixed elevation angle of  $18^\circ$  with a 3 MHz frequency-step  
15 procedure from 3 MHz to 30 MHz; and for a fixed frequency of 15 MHz with a  $5^\circ$  elevation-step  
16 procedure from  $0^\circ$  to  $60^\circ$ .  
17  
18  
19  
20  
21  
22  
23  
24  
25  
26  
27  
28  
29  
30

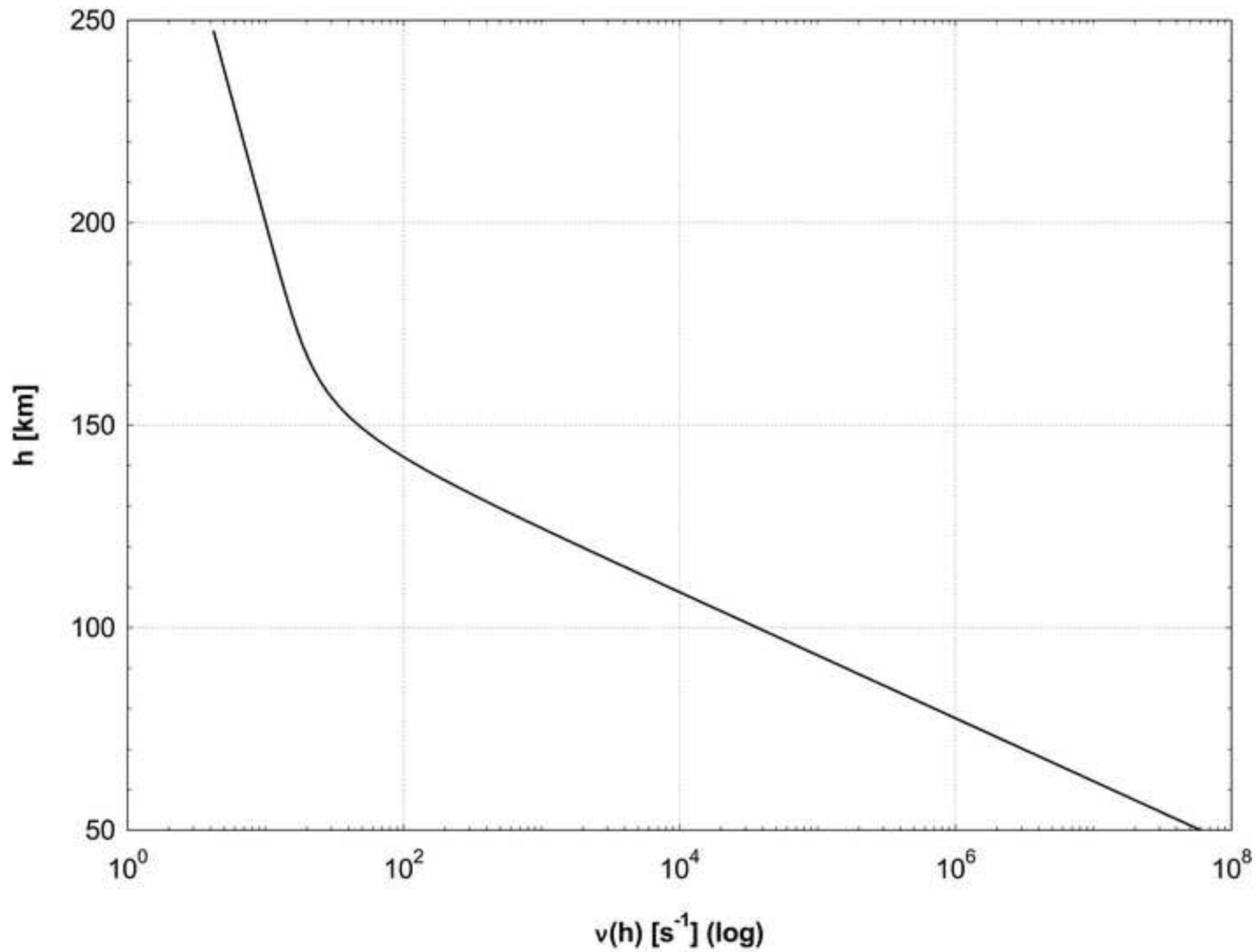
31 **Figure 3.** A comparison between the oblique ionogram recorded over the Rome-Chania radio link  
32 on 07 July 2011 at 15:00 UT (top panel), and the corresponding ionograms synthesized by the  
33 IONORT-IRI-WC (middle panel) and IONORT-ISP-WC (bottom panel) system. The red and  
34 purple vertical lines indicate the MUF values for the 1-hop and 3-hop paths respectively. The LOF  
35 values are also indicated for the E and F regions. For the sake of clarity, only the ordinary trace  
36 computed taking the geomagnetic field into account is shown. Both with single and multiple  
37 ionospheric reflections (1 – 3 hop paths), a nested loop cycle was iterated with azimuth angles from  
38  $121^\circ$  to  $122^\circ$  of step  $0.2^\circ$ . The elevation angle step was set to  $0.2^\circ$  and the RX range accuracy to 0.1  
39 %. The ionograms calculated without applying the collisional model of Eq. 1, labelled with NC are  
40 also shown for a further comparison.  
41  
42  
43  
44  
45  
46  
47  
48  
49  
50  
51  
52  
53  
54  
55  
56  
57

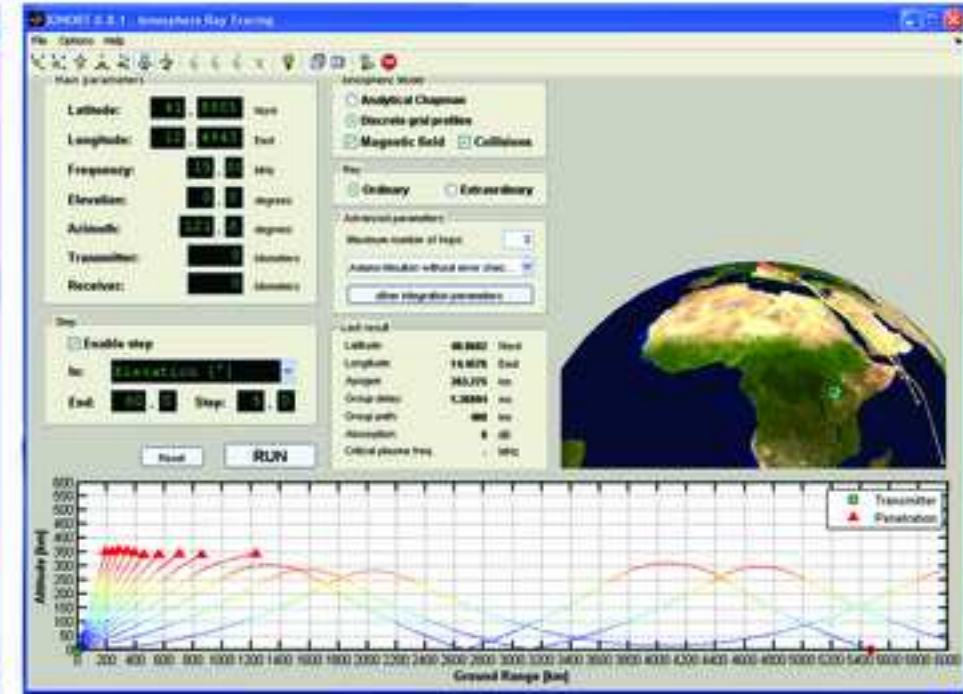
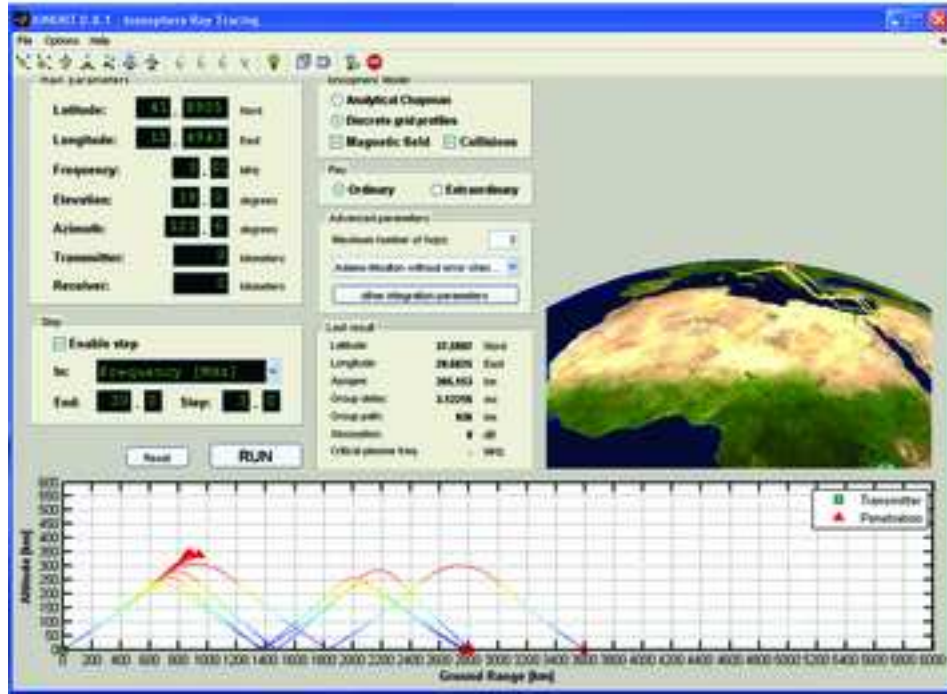
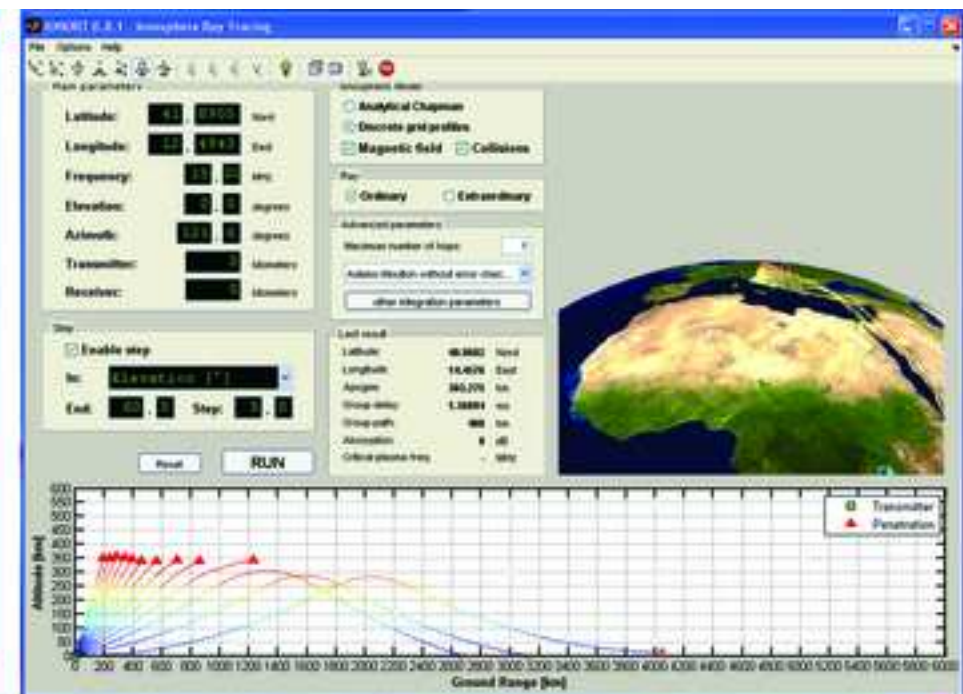
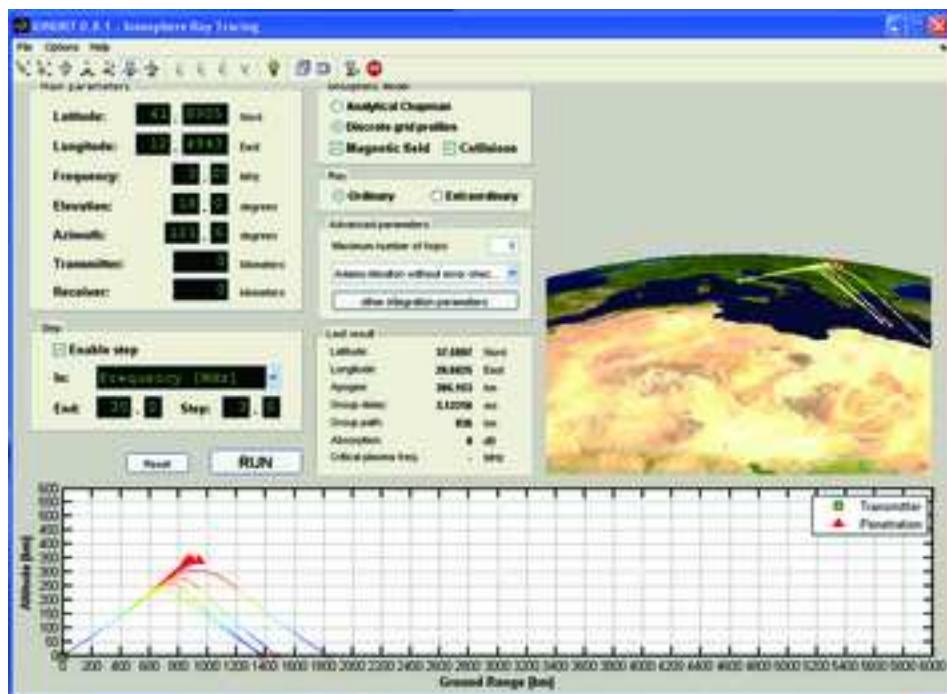
58 **Figure 4.** Same as in Fig. 3. A comparison is shown between the ordinary traces of the oblique  
59 ionograms recorded over the Rome-Chania radio link on 09 October 2011 at 03:00 UT (top panel,  
60  
61  
62  
63  
64  
65

1 on the left), and 26 June 2011 at 01:00 UT (top panel, on the right), and the corresponding  
2 ionograms synthesized by the IONORT-IRI-WC (middle panels) and IONORT-ISP-WC (bottom  
3 panels) system. The ionograms calculated without applying the collisional model of Eq. 1, labelled  
4 with NC are also shown for a further comparison.  
5  
6  
7  
8  
9

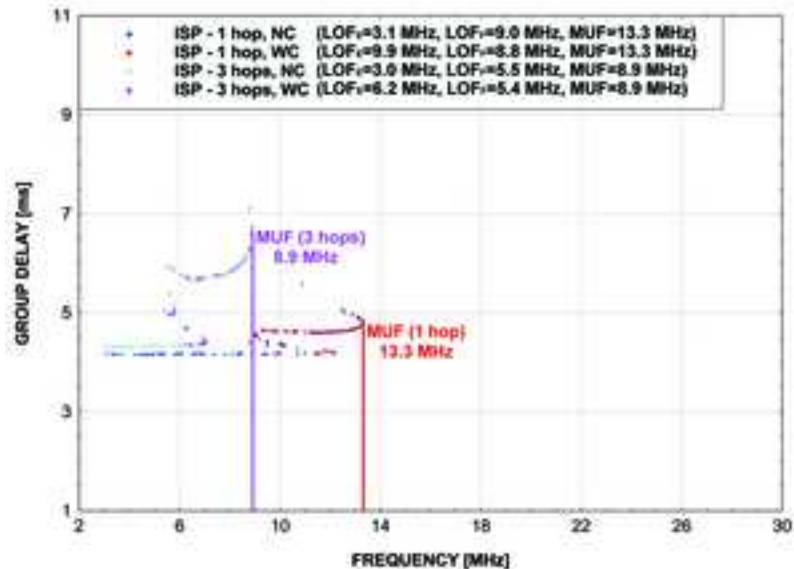
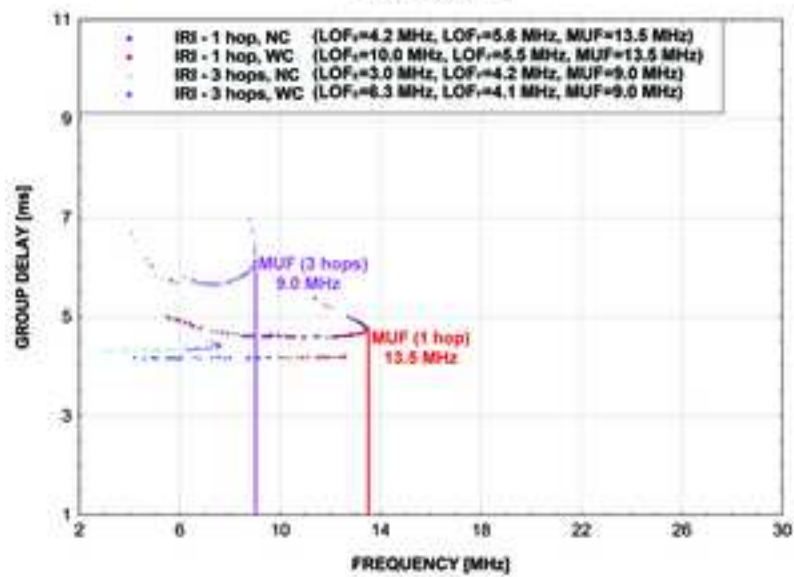
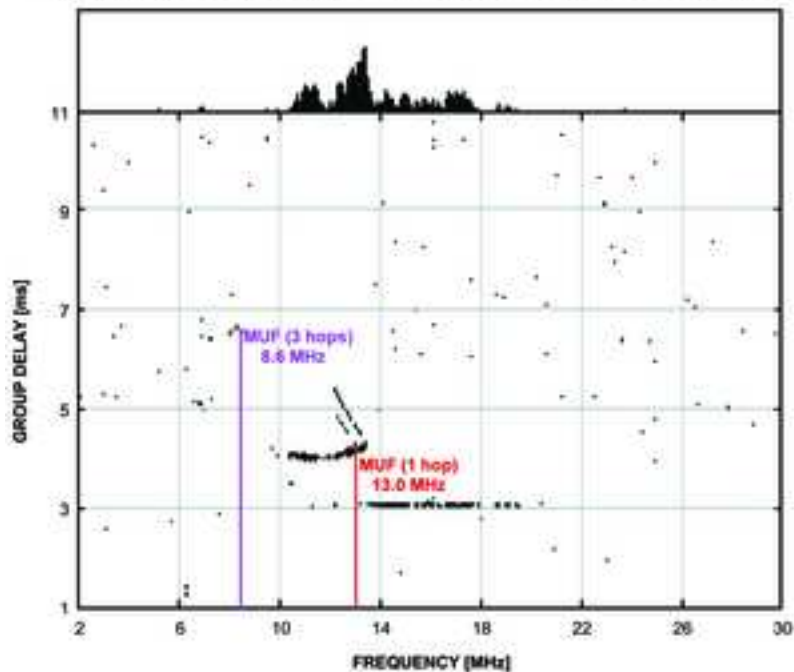
10  
11 **Figure 5.** Comparisons between the differences (IONORT-IRI-WC MUF – measured MUF) (green  
12 squares) and (IONORT-ISP-WC MUF – measured MUF) (red squares) for the whole test database.  
13  
14 The arrows indicate the cases for which the IONORT-ISP-WC system mostly  
15 underestimates/overestimates the MUF values. The symbol \* marks the 6 cases for which  
16 IONORT-IRI-WC system performs better than IONORT-ISP-WC system.  
17  
18  
19  
20  
21  
22  
23  
24  
25

26 **Table 1.** The MUF values calculated by the IONORT-IRI-WC system (column A), the MUF values  
27 calculated by the IONORT-ISP-WC system (column B), the measured MUF values (column C), the  
28 differences IONORT-IRI-WC MUF – measured MUF ( $\Delta_{\text{IRI}}$ , column D) and IONORT-ISP-WC  
29 MUF – measured MUF ( $\Delta_{\text{ISP}}$ , column E) are shown for all the ionograms in the test database. For  
30 each epoch, the lowest difference in absolute value between the modelled MUF (IONORT-IRI-WC  
31 or IONORT-ISP-WC) and the measured MUF is highlighted in bold.  
32  
33  
34  
35  
36  
37  
38  
39  
40  
41  
42  
43  
44  
45  
46  
47  
48  
49  
50  
51  
52  
53  
54  
55  
56  
57  
58  
59  
60  
61  
62  
63  
64  
65

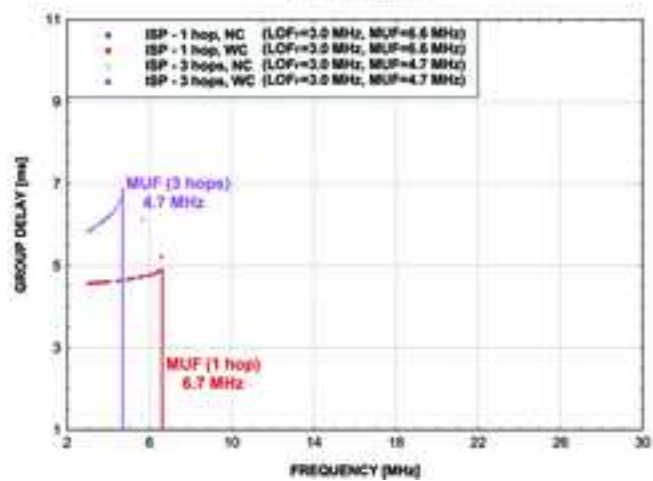
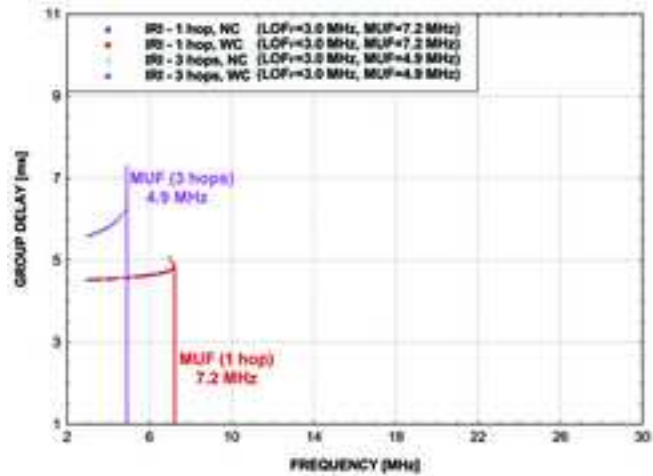
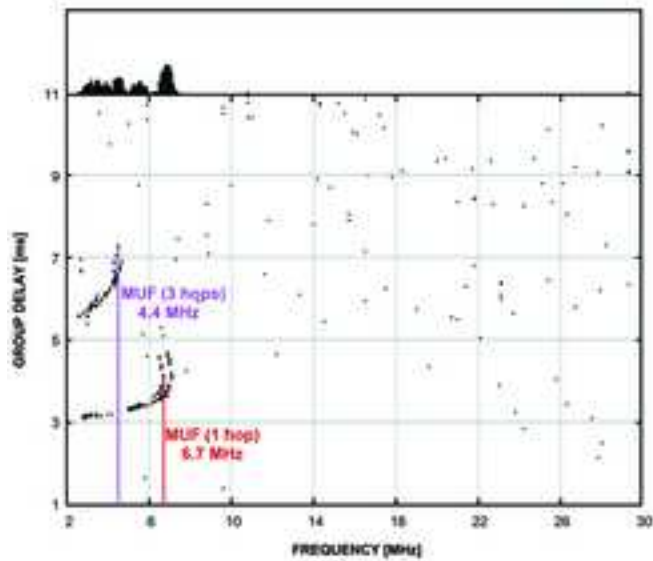




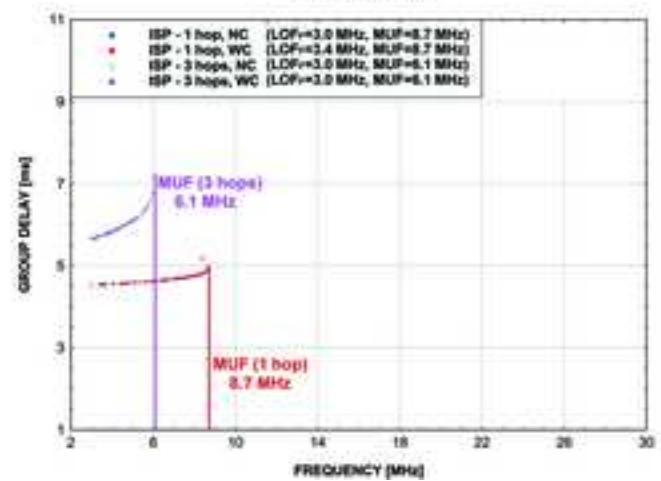
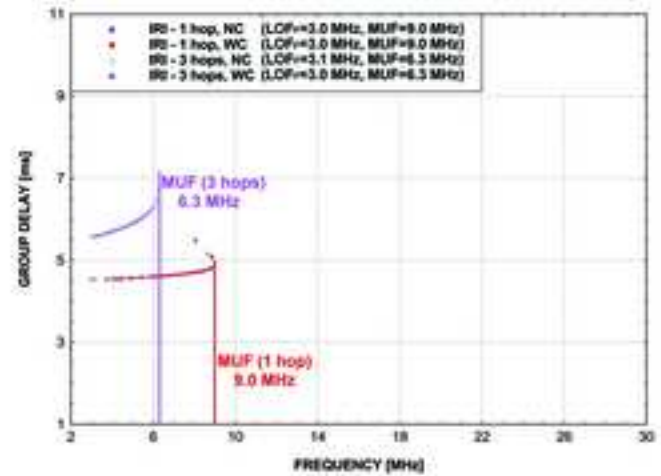
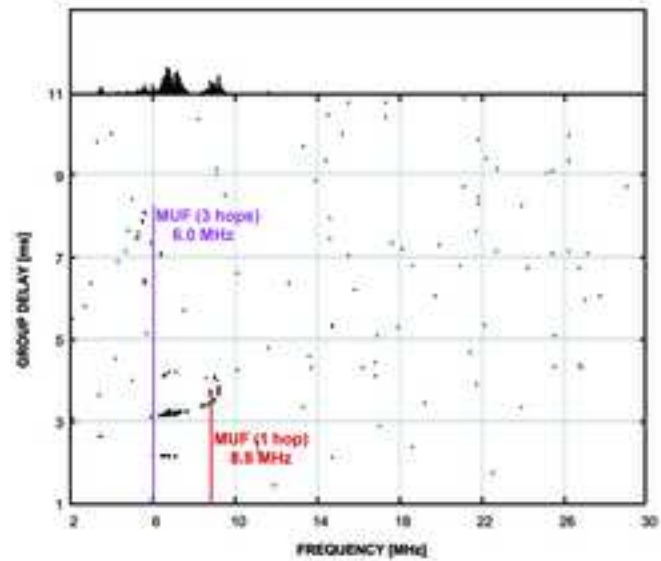
ROME - CHANIA 07 JUL 2011 15:00 UT  
 (NO HORIZONTAL GRADIENTS - with azimuth cycle, elevation step = 0.2°, RX accuracy = 0.1%)

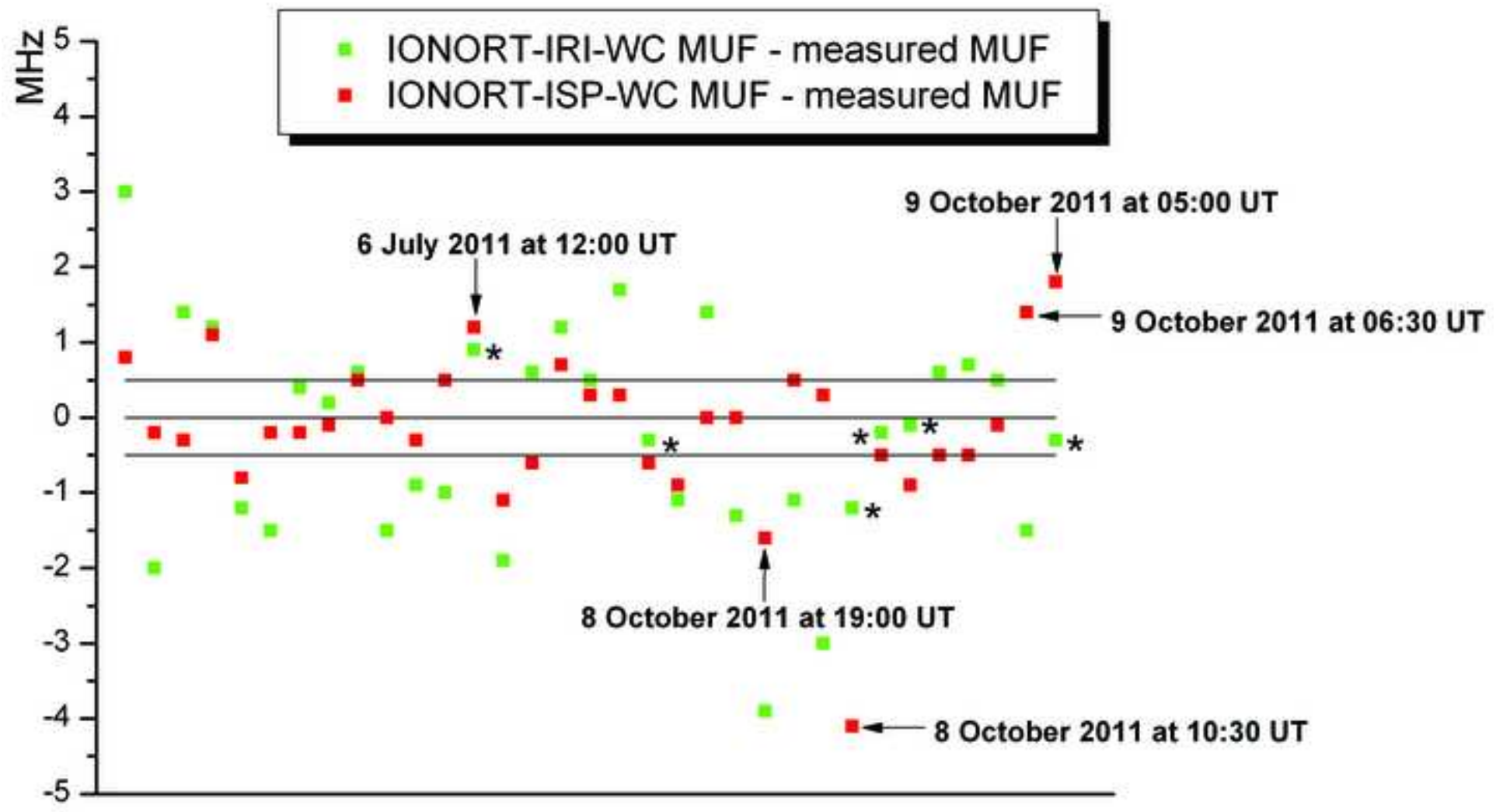


ROME - CHAMA 09 OCT 2011 03:00 UT  
(NO HORIZONTAL GRADIENTS - with azimuth cycle, elevation step = 0.2°, RX accuracy = 0.1%)



ROME - CHAMA 26 JUN 2011 01:00 UT  
(NO HORIZONTAL GRADIENTS - with azimuth cycle, elevation step = 0.2°, RX accuracy = 0.1%)







Epoch	A	B	C	D	E
	IONORT-IRI-WC MUF [MHz]	IONORT-ISP-WC MUF [MHz]	MEASURED MUF [MHz]	$\Delta_{IRI}$ [MHz]	$\Delta_{ISP}$ [MHz]
23 JUN 2011 - 17:00	13.7	11.5	10.7	3.0	<b>0.8</b>
23 JUN 2011 - 19:00	12.9	14.7	14.9	-2.0	<b>-0.2</b>
23 JUN 2011 - 23:00	10.0	8.3	8.6	1.4	<b>-0.3</b>
25 JUN 2011 - 10:00	14.6	14.5	13.4	1.2	<b>1.1</b>
25 JUN 2011 - 20:00	12.2	12.6	13.4	-1.2	<b>-0.8</b>
25 JUN 2011 - 23:00	9.9	11.2	11.4	-1.5	<b>-0.2</b>
26 JUN 2011 - 00:00	9.4	8.8	9.0	0.4	<b>-0.2</b>
26 JUN 2011 - 01:00	9.0	8.7	8.8	0.2	<b>-0.1</b>
26 JUN 2011 - 02:00	8.8	8.7	8.2	0.6	<b>0.5</b>
03 JUL 2011 - 17:00	13.6	15.1	15.1	-1.5	<b>0.0</b>
04 JUL 2011 - 19:00	12.9	13.5	13.8	-0.9	<b>-0.3</b>
04 JUL 2011 - 20:00	12.2	13.7	13.2	-1.0	<b>0.5</b>
06 JUL 2011 - 12:00	14.6	14.9	13.7	<b>0.9</b>	1.2
06 JUL 2011 - 21:00	11.6	12.4	13.5	-1.9	<b>-1.1</b>
07 JUL 2011 - 01:00	8.9	7.7	8.3	0.6	-0.6
07 JUL 2011 - 14:00	13.6	13.1	12.4	1.2	<b>0.7</b>
07 JUL 2011 - 15:00	13.5	13.3	13.0	0.5	<b>0.3</b>
07 JUL 2011 - 17:00	13.5	12.1	11.8	1.7	<b>0.3</b>
07 JUL 2011 - 18:00	13.2	12.9	13.5	<b>-0.3</b>	-0.6
07 JUL 2011 - 19:00	12.9	13.1	14.0	-1.1	<b>-0.9</b>
08 JUL 2011 - 17:00	13.5	12.1	12.1	1.4	<b>0.0</b>
08 JUL 2011 - 18:00	13.2	14.5	14.5	-1.3	<b>0.0</b>
08 JUL 2011 - 19:00	12.8	15.1	16.7	-3.9	<b>-1.6</b>
08 OCT 2011 - 06:15	14.8	16.4	15.9	-1.1	<b>0.5</b>
08 OCT 2011 - 06:45	14.7	18.0	17.7	-3.0	<b>0.3</b>
08 OCT 2011 - 10:30	19.3	16.4	20.5	<b>-1.2</b>	-4.1
08 OCT 2011 - 20:00	9.0	8.7	9.2	<b>-0.2</b>	-0.5
08 OCT 2011 - 23:45	7.6	6.8	7.7	<b>-0.1</b>	-0.9
09 OCT 2011 - 02:00	7.5	6.4	6.9	0.6	<b>-0.5</b>
09 OCT 2011 - 02:15	7.5	6.3	6.8	0.7	<b>-0.5</b>
09 OCT 2011 - 03:00	7.2	6.6	6.7	0.5	<b>-0.1</b>
09 OCT 2011 - 05:00	10.7	13.6	12.2	-1.5	<b>1.4</b>
09 OCT 2011 - 06:30	14.8	16.9	15.1	<b>-0.3</b>	1.8